Lung-Specific Delivery of Paclitaxel by Chitosan-Modified PLGA Nanoparticles Via Transient Formation of Microaggregates

RUI YANG,[1,2,3] SU-GEUN YANG,[1,2] WON-SIK SHIM,[1,2] FUDE CUI,[3] GANG CHENG,[3] IN-WHA KIM,[1,2] DAE-DUK KIM,[2] SUK-JAE CHUNG,[2] CHANG-KOO SHIM[1,2]

[1]National Research Laboratory for Transporters Targeted Drug Design, College of Pharmacy, Seoul National University, Seoul 151-742, Korea

[2]Research Institute of Pharmaceutical Sciences, College of Pharmacy, Seoul National University, Seoul 151-742, Korea

[3]Department of Pharmaceutics, College of Pharmacy, Shenyang Pharmaceutical University, Shenyang 110016, China

Received 3 March 2008; revised 16 May 2008; accepted 5 June 2008

Published online 25 July 2008 in Wiley InterScience (www.interscience.wiley.com). DOI 10.1002/jps.21487

ABSTRACT: Chitosan-modified paclitaxel-loaded poly lactic-*co*-glycolic acid (PLGA) nanoparticles with a mean diameter of 200–300 nm in distilled water were prepared by a solvent evaporation method. The mean diameter increased dramatically in contact with the mouse (CDF_1) plasma, as a function of chitosan concentration in the modification solution (e.g., 2670.5 nm for 0.7% chitosan-modified nanoparticles, NP_3), but reverted to almost its original size (i.e., 350.7 nm for NP_3) following 5 min of gentle agitation. The zeta potential of PLGA nanoparticles was changed to positive by the chitosan modification. The *in vitro* uptake into, and cytotoxicity of the nanoparticles against, a lung cancer cell line (A549) were significantly increased by the modification. Most importantly, a lung-specific increase in the distribution index of paclitaxel (i.e., AUC_{lung}/AUC_{plasma}) was observed for chitosan-modified nanoparticles (e.g., 99.9 for NP_3 vs. 5.4 for Taxol™) when nanoparticles were administered to lung-metastasized mice via the tail vein at a paclitaxel dose of 10 mg/kg. Transient formation of aggregates in the blood stream followed by enhanced trapping in the lung capillaries, and electrical interaction-mediated enhanced uptake across the endothelial cells of the lung tumor capillary appear to be responsible for the lung-tumor-specific distribution of the chitosan modified nanoparticles. © 2008 Wiley-Liss, Inc. and the American Pharmacists Association J Pharm Sci 98:970–984, 2009

Keywords: transient aggregates; nanoparticles; poly(lactic/glycolic)acid (PLGA); paclitaxel; chitosan; surface modification; capillary; distribution; lung; cancer

INTRODUCTION

Lung cancer is the most common cause of death from cancer, with an annual toll of 1.18 million deaths.[1] Non-small lung cancer (NSCLS) accounts for 70–80% of lung cancer diagnoses and the disease is generally diagnosed at an advanced stage. A combination of surgery and chemotherapy is the traditional treatment method, but the long-term survival of patients with NSCLS is low, typically less than 5% at 5 years. Furthermore, the toxicity of chemotherapy to non-target tissue represents a strict limit to the use of doses high enough to achieve potential further improvement in survival.[2] Therefore, non-selectivity of the

Correspondence to: Chang-Koo Shim (Telephone: +82-2-880-7873; Fax: +82-2-888-5969; E-mail: shimck@snu.ac.kr)

Journal of Pharmaceutical Sciences, Vol. 98, 970–984 (2009)

currently available anticancer drugs is a commonly encountered problem that reduces therapeutic efficacy.

Two lung-specific strategies have been developed so far: microspheres and inhalation. Microspheres, with particle sizes ranging from 5 to 15 μm, have been extensively investigated. They were able to block the alveolar capillary barrier for a long time and were then taken up by the alveolar macrophages. However, particles with diameter >5 μm may block the blood capillaries and cause chronic obstructive pulmonary emphysema.[3] The microparticles may also result in arterial embolization after intravenous administration.[4] Therefore, the safety of lung-targeting microspheres remains uncertain. Recently, pulmonary inhalation has been actively investigated. However, some disadvantages exist, such as the high production cost, instability during storage,[5] and disruption and premature loss of the entrapped substance during nebulization.[6] Moreover, the route is inappropriate for use with large dose drugs[7] and frequent inhalation could induce lung fibrosis.[8,9] Therefore, it is necessary to develop novel lung-specific drug delivery systems that can overcome these drawbacks.

Organ-specific delivery of anticancer drugs following systemic administration appears to be achievable by simple modification of the surface characteristics with certain materials.[10,11] In the present study, we examined the feasibility of chitosan-modified PLGA nanoparticles[12] as a lung-specific system for delivery of paclitaxel for the treatment of lung cancers by intravenous. Paclitaxel, a novel anticancer drug originating from the bark of the pacific yew, is one of the first-line treatment drugs for advanced NSCLS. Taxol™ is the only dosage form of paclitaxel currently available. However, Cremophor EL™ (polyethoxylated castor oil), a material that results in many serious side effects, such as hypersensitivity reactions, nephrotoxicity, neurotoxicity, and cardiotoxicity,[13] is used as a solubilizer of paclitaxel in the formulation. Various advanced formulation strategies, such as utilizing cosolvent systems,[14] parenteral emulsions,[15] micells,[16] liposomes,[17] microspheres,[18] and inclusion complexes[19] have been tried, but have not been particularly successful in delivering paclitaxel to lung tumors.

The fundamental objective of the present study, therefore, was to develop a PLGA nanoparticle system that can efficiently deliver anticancer drugs, such as paclitaxel, to lung tumors in cancer patients. PLGA and chitosan were chosen based on their biodegradable and biocompatible characteristics.[20,21] Chitosan, a cationic polyelectrolyte, was selected as a surface modifying material in this study, since it provides a strong electrical interaction with the negative charge of the PLGA nanoparticle surface, changing the surface to a positive charge. The cationic nanoparticles are supposed to be selectively taken up by the tumor vasculature endothelial cells.[22] In addition, considering that cell membranes, particularly cancer cell membranes, are negatively charged,[23,24] the positive surface charge of nanoparticles would be favorable for the endocytosis of nanoparticles into the cancer cell. Moreover, the positive surface charge induced by the chitosan modification may accelerate clathrin-mediated endocytosis of nanoparticles.[25] The adhesive characteristics of chitosan may enhance the adherence of nanoparticles to the cell surface,[26,27] thereby accelerating the phagocytosis of nanoparticles into the cell.

MATERIALS AND METHODS

Materials

Paclitaxel was purchased from Taihua National Plant Pharmaceutical Corporation (Shan Xi, China). PLGA with a lactide/glycolide molar ratio of 50:50 (MW = 40000–75000), polyvinyl alcohol (PVA, MW = ~67000), chitosan (MW = 45500–50000, deacetylation degree = 75–80%), coumarin-6 (MW = 350.43), RPMI 1640 cell culture medium (powder with L-glutamine and without sodium bicarbonate, developed at Roswell Park Memorial Institute) and phosphate-buffered saline (PBS, pH 7.4, 0.01 M) were purchased from Sigma–Aldrich (St. Louis, MO). A human lung cancer cell line, A549, was purchased from a Korea cell line bank (Seoul, Korea). Dichloromethane (extra pure) was purchased from Dae Jine Chemical Co. Ltd. (Kyeongnam, Korea). All other chemicals were the highest grade possible and obtained from commercial sources.

Animals

Male CDF1 mice weighting 18–22 g, 3–4 weeks old and male SD rats weighing 250 g were purchased from the Central Lab Animal Inc. (Seoul, Korea). All animal experiments were performed according to the Guidelines in Animal Care and Use of Seoul National University, Seoul, Korea.

METHODS

Preparation of Surface-Modified PLGA Nanoparticles

PLGA nanoparticles containing paclitaxel were prepared using a solvent evaporation method.[28] Briefly, a dichloromethane solution (2 mL) containing PLGA (47.5 mg) and paclitaxel (2.5 mg) was poured into a glass bottle containing a 4% (w/v) water solution of PVA (10 mL), and the mixture was sonicated for 1 min (Model 100, Fisher Scientific Inc., Pittsburg, PA). The mixture was then poured into a 50 mL glass beaker containing a 1% (w/v) water solution of PVA (40 mL) under magnetic stirring at 40°C. After overnight stirring, the resulting PLGA dispersion was transferred to a 50 mL centrifuge tube (Corning Inc., New York, NY) and centrifuged at 919.7*g* for 10 min. The resulting supernatant was transferred to ultracentrifuge tubes (Beckmann Instruments, Fullerton, CA) and further centrifuged at 41137.3*g* for 20 min to separate the nanoparticles. The sediment obtained was resuspended in double distilled water (DDW, 50 mL) with the aid of a sonicator and centrifuged at 41137.3*g* for 20 min. This process (i.e., resuspension of sediment and centrifugation) was repeated twice to wash out PVA, which is not allowed for use as an intravenous excipient. The resulting dispersion was then freeze dried (Bondiro, Ilshin Lab. Co., Seoul, Korea) at −100°C for 1 day. The nanoparticles obtained (i.e., NP_0 in Table 1) were stored in the centrifuge tube at −10°C for further experiments.

Chitosan-modified PLGA nanoparticles containing paclitaxel (i.e., NP_1, NP_2, and NP_3 in Tab. 1) were prepared as follows: a chitosan stock solution was prepared by dissolving chitosan in 1% (w/v) acetic acid, and appropriately diluted with DDW to yield 0.3%, 0.5%, and 0.7% (w/v) solutions. To 10 mL of each chitosan solution, PLGA nanoparticles (i.e., NP_0) were redispersed under sonication and mixed overnight by magnetic stirring at room temperature. The suspension was then ultracentrifuged at 92566.5*g* for 50 min at 4°C, and the resulting supernatant layer was removed by decantation. The remaining sediment was resuspended in DDW (50 mL) with the aid of a sonicator. The process described above was repeated twice and the final sediment was freeze-dried. Nanoparticles modified with the 0.3%, 0.5%, and 0.7% chitosan solutions were designated as NP_1, NP_2, and NP_3, respectively.

Table 1. Physical Characteristics of Paclitaxel-Loaded PLGA Nanoparticles (NP_0) and Chitosan-Modified, Paclitaxel-Loaded PLGA Nanoparticles (NP_1, NP_2, and NP_3) in DDW and Fresh Mouse (CDF_1) Plasma (mean ± SD, n = 3)

Formulations (Chitosan Concentration in the Modification Solution, w/v %)	DDW			Plasma			Loading Efficiency (%)	Drug Content (%)
	Particle Size (nm)	Polydispersity	Zeta Potential (mV)	Particle Size (nm)	Polydispersity	Zeta Potential (mV)		
NP_0 (0)	202.11 ± 2.34	0.11 ± 0.02	−28.42 ± 3.04	237.82 ± 58.32	0.21 ± 0.06	−29.71 ± 4.64	70.21 ± 3.53	3.51 ± 0.18
NP_1 (0.3)	240.64 ± 3.21	0.15 ± 0.04	+8.91 ± 2.02	600.91 ± 72.14	0.38 ± 0.12	+3.57 ± 1.51	71.82 ± 3.21	3.59 ± 0.16
NP_2 (0.5)	252.12 ± 2.53	0.20 ± 0.03	+17.31 ± 2.42	1289.53 ± 135.64	0.40 ± 0.17	+10.83 ± 2.91	68.73 ± 2.61	3.44 ± 0.13
NP_3 (0.7)	280.62 ± 3.61	0.16 ± 0.04	+31.83 ± 1.81	2670.51 ± 319.93	0.58 ± 0.30	+20.92 ± 5.94	69.62 ± 2.94	3.48 ± 0.15

DOI 10.1002/jps

To examine the *in vitro* cellular uptake of nanoparticles, coumarin 6, instead of paclitaxel, was used in the preparation of PLGA nanoparticles, with and without chitosan modification in the same manner that was described for the paclitaxel nanoparticles.

Physical Characterization of Nanoparticles

The particle size, size distribution and surface charge of the nanoparticles were measured by electrophoretic light scattering spectrophotometry (ELS-8000, Otsuka Electronics Co. Ltd., Osaka, Japan), based on dynamic light scattering, after appropriate dilution of the nanoparticles with DDW. The surface morphology of the nanoparticles was visualized by scanning electron microscopy (SEM, JSM-5600, Jeol Co., Tokyo, Japan) at 35000× magnification after a platinum coating of nanoparticles for 40 s using an ion sputter coater (JFC-1100, Joel Co., Tokyo, Japan). X-ray diffractometry (D-5005, Siements, Karlsruhe, Germany) was conducted to examine the existing status of the paclitaxel in the nanoparticles. The diffraction angle (2θ) was recorded from 0° to 64° with a scanning speed of 3°/min.

The characteristics of nanoparticles measured in DDW may change in the stream of plasma *in vivo*.[29] Thus, the size, as well as the zeta potential, was measured again after pre-incubation of the nanoparticles at 37°C for 30 min with fresh mouse (CDF_1) plasma under shaking at 120 rpm. Nanoparticles were collected by the centrifugation of the incubation medium at 15600*g* for 3 min, redispersed in DDW, and measured for size and zeta potential.

Nanoparticles in distilled water (DDW) or in plasma were appropriately diluted with DDW, dropped on formvar-coated copper grids (300-mesh, hexagonal fields), air dried for 5 min at room temperature, stained with a 2% uranyl acetate solution (10 μL), air-dried again for 10 min at room temperature, and then observed for the morphology by transmission electron microscopy (TEM, JEM-1010, Jeol Co.).

Determination of Loading Efficiency of Paclitaxel

To determine the loading efficiency of paclitaxel in nanoparticles, nanoparticles (approximately 1.5 mg) were dissolved in 0.5 mL dichloromethane and mixed with 2 mL of an acetonitrile/water solution (50:50, v/v). The mixture was then vortexed vigorously for 5 min, and dichloromethane was evaporated under a nitrogen stream until a clear solution was obtained. The paclitaxel in the solution was measured by HPLC after appropriate dilution with a mixture of acetonitrile and water (50:50, v/v). The loading efficiency (%) of paclitaxel was calculated using the following equation:

$$\text{Loading efficiency}\,(\%) = \frac{\text{amount of paclitaxel recovered from nanoparitcles}}{\text{amount of paclitaxel used in preparation of nanoparticles}} \times 100$$

In Vitro Release of Paclitaxel

In vitro release of paclitaxel from nanoparticles was measured according to a previous method[30] after minor modification. Nanoparticles (10 mg) were diluted with 10 mL of phosphate-buffered saline (PBS, pH 7.4, 0.01 M) or fresh SD rat plasma in a capped centrifuge tube, and gently shaken at 120 rpm in an orbital shaker in a water bath (37°C). At specified time points during 6–220 h period, the tube was taken out of the shaker and centrifuged at 41137.3*g* for 20 min. The resulting pellet was resuspended in 10 mL of fresh release medium (i.e., PBS or plasma) and placed back into the water bath for continuous release studies. The supernatant from the PBS sample was collected and extracted for paclitaxel with dichloromethane (1.0 mL). After the removal of dichloromethane by nitrogen flow, the deposited paclitaxel was dissolved in 2.0 mL of the mobile phase, a mixture of acetonitrile and water (50:50, v/v), and filtered using 0.2 μm membrane filters, 20 μL aliquots of the filtrate were injected directly into the HPLC column.

The supernatant from the plasma sample was collected, spiked with 100 μL of *n*-butyl *p*-hydroxy benzoate (25 μg/mL, internal standard for HPLC), extracted for paclitaxel with 4 mL of ethyl acetate with vigorous mixing for 5 min, and the mixture was centrifuged at 892.6*g* for 5 min. The extraction procedure was repeated twice, and the organic phases were combined and dried under

nitrogen gas. The residue was then dissolved with 150 μL of the mobile phase, filtered using 0.2 μm membrane filters and a 100 μL aliquot was injected into the HPLC column.

The HPLC assay of paclitaxel was performed according to a reported method.[31] The HPLC system was equipped with an HPLC column (a reverse phase Resolve™ Spherical C18 column: 3.9 mm × 150 mm, 5 μm) in an HPLC system (Waters, 2487 Dual λ absorbance detector, 717 plus autosampler and 515 HPLC dual pumps, Milford, MA). The detector wavelength was set at 227 nm. The mobile phase, a mixture of acetonitrile and water (50:50, v/v), was eluted at a flow rate of 1.0 mL/min.

Cellular Uptake of Coumarin 6 from Nanoparticles

To examine the effect of the surface modification with chitosan on the cellular uptake of the nanoparticles, an *in vitro* uptake experiment was performed for coumarin 6-loaded PLGA nanoparticles using A549 cells. Coumarin 6 was selected as a model compound based on its high sensitivity of determination in the cell. The cells were routinely grown at 37°C with an RPMI 1640 medium, supplemented with 10% fetal bovine serum (FBS), 100 IU/mL penicillin, 100 μg/mL streptomycin and 2 mM L-glutamine (both from Welgene Inc., Daegu, Korea) in a 5% CO_2/95% air humidified atmosphere. The cells were seeded into 96-well microplates (Black Clear Bottom Cell Culture Microplates 3603, Corning Costar Corp., Cambridge, MA) at a cellular density of 1×10^4 cells/well. When 80% confluence was reached, the medium was replaced by 100 μL of fresh mouse (CDF_1) plasma containing coumarin 6-loaded PLGA nanoparticles (0.25 mg/mL), and the plates were incubated for 2 h at 37°C and 60 rpm. The content of coumarin 6 in all the nanoparticles was identical at 3.5% (w/w). The incubation was terminated by the addition of ice-cold PBS (100 μL), and the PBS was removed. This process was repeated twice to eliminate nanoparticles that were not taken up by the cells. The cell membrane was then lysed with 100 μL of 0.5% triton X-100 solution in 0.2 N NaOH, and the concentration of coumarin 6 in the lysate was determined using a microplate reader (Synergy HT, BioTek Instruments, Winooski, VT) at excitation and emission wavelengths of 430 and 485 nm, respectively.

In Vitro Cytotoxicity Assay

A549 cells were transferred to 96-well plates at a cellular density of 1×10^4 cells per well as described above for the uptake study. When 80% confluence was reached in each well (Corning Costar Corp.), the medium was replaced by 100 μL fresh mouse (CDF_1) plasma containing 1, 2, or 4 μg paclitaxel or paclitaxel-loaded nanoparticles with equivalent amounts of paclitaxel. One row of the 96-well plates was subjected to the control study, in which a culture medium without the drug or nanoparticles was tested. The plates were then incubated for 24, 48, and 72 h. At specified time points, the medium was removed and the wells were washed three times with PBS (100 μL). One hundred microliters of 3-(4,5-dimethylthiazol-2-yi)-2,5-diphenyltetrazolium (MTT assay solution), which was prepared by mixing 10 μL of MTT stock solution (5 mg/mL) and 90 μL of incubation medium, was added to each well and incubated for 3 h. After incubation, the medium was removed, and dimethylsufoxide (DMSO, 100 μL) was added to the remaining precipitates on the plates in the well. The absorbance of the resulting DMSO solution was determined at 560 nm using a microplate reader (Molecular Devices Co., Sunnyvale, CA). The percentage of cell viability was calculated using the following equation:

$$\text{Cell viability}\,(\%) = \frac{\text{Abs}_{\text{test cells}}}{\text{Abs}_{\text{control cells}}} \times 100$$

where $\text{Abs}_{\text{test cells}}$ and $\text{Abs}_{\text{control cells}}$ represent absorbances for the cells treated with paclitaxel or nanoparticles and the cells treated with the culture medium, respectively.

Pharmacokinetics and Biodistribution Studies of Paclitaxel

Pharmacokinetics and biodistribution of paclitaxel were investigated in normal and lung metastasized CDF_1 mice. The lung metastasis was induced by tail vein injection of CT-26 cells, a transplantable mouse colon cancer cell line, routinely grown with RPMI 1640 medium supplemented with 10% FBS, 100 IU/mL penicillin, 100 μg/mL streptomycin, and 2 mM L-glutamine in 5% CO_2 humidified air at 37°C, to CDF_1 mice at a concentration of 1×10^5 cells/mouse.[32] Exactly 2 weeks after the injection of CT-26 cells, the mice were subjected to the pharmacokinetics and biodistribution studies.

Taxol™, chitosan-unmodified paclitaxel-loaded nanoparticles (NP_0), and chitosan (0.7%)-modified paclitaxel-loaded nanoparticles (NP_3) were injected to mice at a paclitaxel dose of 10 mg/kg, and the plasma, heart, liver, spleen, lung, and kidney were harvested at 5 min, 30 min, 2 h, 4 h, 6 h, 8 h, and 12 h after the administration of each formulation. Blood samples were taken from the eye, and centrifuged in Eppendorf tubes at 4°C to collect plasma samples. The organs were washed twice with physiological saline (0.9% sodium chloride) and blotted dry. Plasma and tissue samples were stored at −50°C for paclitaxel analysis. Four mice were euthanized at each of the seven sampling time points for each formulation (i.e., a total of 28 mice for each formulation).

For the assay of paclitaxel in the plasma, 150 μL plasma sample was spiked with 50 μL *n*-butyl *p*-hydroxy benzoate (25 μg/mL, internal standard), extracted with 2 mL of ethyl acetate with vigorous mixing for 5 min, and the mixture was centrifuged at 892.6*g* for 5 min. The extraction procedure was repeated twice, and the organic phases were combined and dried under nitrogen gas. The residue was then dissolved with 150 μL of the mobile phase, and a 100 μL aliquot was injected into the HPLC column.

For the assay of tissue samples, each tissue was homogenized for 5 min at 4°C with 4 times the volume of water containing 4% (w/v) bovine serum albumin using a tissue homogenizer (IEA-Ultra-Turrax® T25 basic, Germany). The tissue homogenate was spiked with 50 μL internal standard (*n*-butyl *p*-hydroxy benzoate, 25 μg/mL) and extracted twice with 2 mL of ethyl acetate each time, as described above for plasma samples. The ethyl acetate fractions were combined and dried under nitrogen gas. The residue was reconstituted with 150 μL of the mobile phase, and 100 μL aliquot was injected into the HPLC column. The HPLC equipment and assay condition were identical to those described in the *in vitro* release test.

The area under the plasma or tissue concentration–time curve from time zero to infinity (AUC), plasma systemic clearance (CL) and distribution volume at steady state (Vd_{ss}) of paclitaxel were calculated using WinNonlin software (Pharsight, Mountain View, CA).

Statistical Analysis

All data were expressed in the form of the mean ± SD when possible. Data were analyzed for statistical significance by one-way analysis of variance (ANOVA) followed by Sheffe's test. Values of $p < 0.001$ or $p < 0.05$ were considered significant.

RESULTS AND DISCUSSION

Physical Characteristics of Nanoparticles

The physical characteristics of nanoparticles were measured in DDW and plasma and are summarized in Table 1. The loading efficiency and content of paclitaxel in the nanoparticles were kept in the range of 69.62–71.82% and 3.44–3.59%, respectively, regardless of chitosan modification. On the other hand, the size and zeta potential of nanoparticles in DDW were significantly influenced by the modification. The size of nanoparticles increased as the concentration of chitosan in the modification solution increased, but continued to be smaller than 300 nm. The zeta potential of nanoparticles changed to positive, in parallel with the chitosan concentration. This is consistent with the coating of the PLGA nanoparticle (NP_0) surface, which is negative due to the presence of polymeric carboxylic groups[33,34] with the positively charged chitosan molecules.

The size measured *in vitro* may be very different from the actual size in systemic circulation, because an increase of up to 50% in the size is generally observed for nanoparticles due to aggregation or opsonization upon contact with a protein-containing medium.[29] Consistent with this report, the size of PLGA nanoparticles as well as the polydispersity index increased in contact with plasma in the present study. Most importantly, the size of nanoparticles increased dramatically as the concentration of chitosan in the modification solution increased (i.e., in the order of NP_0, NP_1, NP_2 and NP_3). For example, the size of NP_3 increased up to 2670.51 nm (2.7 μm), a 9.5-fold increase compared to that in DDW (Fig. 3A and Tab. 1). Considering that the increase in size was parallel to that of the zeta potential (Tab. 1), it appears that electrical interaction between nanoparticles (+ charged) and plasma proteins (− charged) to form nanoparticle-protein aggregates (Fig. 3) was responsible for the size increase. While the size of nanoparticles in the plasma [e.g., 2.7 μm for NP_3 (Tab. 1)] reverted nearly to their original values in DDW [e.g., to 350.69 ± 50.25 nm (mean ± SD, $n = 3$) after the agitation vs. 280.62 ± 3.61 nm in DDW (Fig. 3B

and Tab. 1) for NP_3] when the aggregates were gently agitated for 5 min with a glass rod. The size reduction may be attributable to the dissociation of aggregates suggesting that the aggregation based on electronic interaction is transient and weak rather than permanent and strong.

X-Ray Diffraction

Figure 1 shows X-ray patterns of paclitaxel powders, chitosan powders, drug-unloaded PLGA nanoparticles (blank NP), chitosan-unmodified paclitaxel-loaded PLGA nanoparticles (NP_0), and chitosan-modified paclitaxel-loaded PLGA nanoparticles (NP_1, NP_2, and NP_3). Paclitaxel-specific peaks, which appeared at about 6° and 12°, disappeared in all the nanoparticles of blank NP, NP_0, NP_1, NP_2, and NP_3, suggesting that paclitaxel in the nanoparticles does not exist as a crystal form, but as an amorphous form.

Morphology of Nanoparticles

The SEM images of nanoparticles are shown in Figure 2. Paclitaxel crystal was not observed for any of the nanoparticles (A–D), consistent with the result of the X-ray study (Fig. 1). The shape of the nanoparticles was spherical and their size was less than 300 nm, consistent with the result of the electrophoretic light scattering spectrophotometry in DDW (Tab. 1). The surface smoothness of the nanoparticles, however, decreased as the chitosan concentration in the modification solution increased in the order of NP_0, NP_1, NP_2, and NP_3, consistent with the existence of sticky chitosan on the surface of the nanoparticles.

TEM images of nanoparticles in the plasma are shown in Figure 3. Figure 3A represents the formation of aggregates, while Figure 3B represent the dissociation of the aggregates by gentle agitation for 5 min with a glass rod.

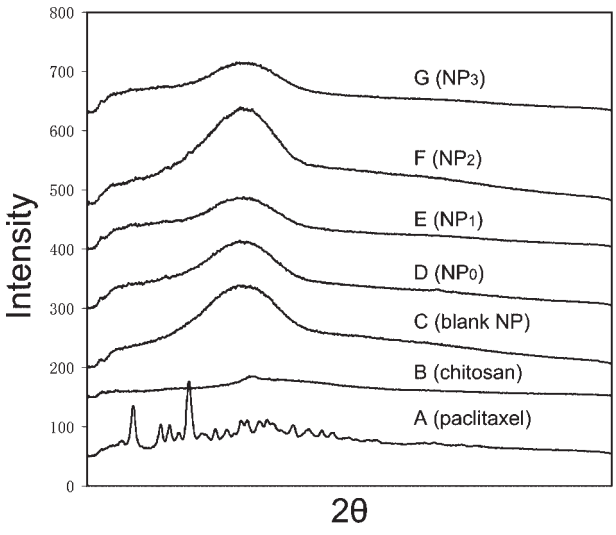

Figure 1. X-ray diffractometry patterns of paclitaxel powder (A), chitosan powder (B), surface-unmodified, drug-unloaded PLGA nanoparticles (blank NP, C), surface-unmodified, paclitaxel-loaded PLGA (NP_0, D), 0.3% chitosan-modified, paclitaxel-loaded PLGA (NP_1, E), 0.5% chitosan-modified, paclitaxel-loaded PLGA (NP_2, F), and 0.7% chitosan-modified, paclitaxel-loaded PLGA nanoparticles (NP_3, G).

Paclitaxel Release from Nanoparticles

The release of paclitaxel from the nanoparticles in PBS and plasma medium are shown in Figure 4. In both release medium, biphasic release behavior was observed for all of the nanoparticles with a faster release phase during the initial period and a slower release phase thereafter. Comparing in the PBS, the all formulation showed a greater burst effect of drug and a following higher cumulative release percentage in rat plasma ($p < 0.05$). Combined with the known fact that the PLGA polymer could be strongly degraded by enzymatic degradation on the polymer surface,[35] it is hypothesized that drug release from the PBS follows diffusion-based model while a diffusion and erosion-controlled pattern in rat plasma. In the initial release phase, where surface bound and poorly encapsulated drug is release, may resulting from diffusion from nanoparticles surface in the PBS medium and from the polymer erosion and diffusion in the biological condition. In the later phase, drug is slower release from the core of the nanoparticles. The similar mechanism is obtained in the poly (methoxy polyethyleneglycol cyanoacrylate-*co*-*n*-hexadecyl cyanoacrylate) nanoparticles.[30] Regardless of dissolution medium, the release was retarded as the concentration in the modification solution increased, suggesting that the chitosan layer on the nanoparticle surface serves as an additional barrier for the diffusion of paclitaxel.

Cellular Uptake of Coumarin 6 from Nanoparticles

Figure 5 shows the cellular uptake of coumarin 6 by A549 cells in 2 h from fresh mouse (CDF_1)

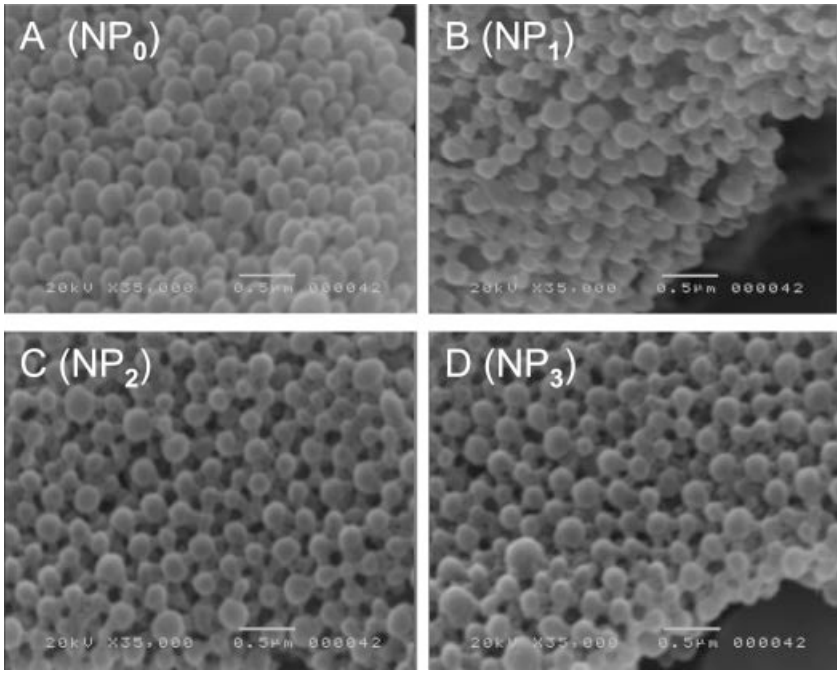

Figure 2. SEM images of surface-unmodified, paclitaxel-loaded PLGA nanoparticles (NP_0, A), 0.3% chitosan-modified, paclitaxel-loaded PLGA nanoparticles (NP_1, B), 0.5% chitosan-modified, paclitaxel-loaded PLGA nanoparticles (NP_2, C), and 0.7% chitosan-modified, paclitaxel-loaded PLGA nanoparticles (NP_3, D).

plasma dispersion of various nanoparticles. Most of the uptake in Figure 5 could be attributable to the uptake of nanoparticles rather than the uptake of released coumarin 6 because the release of coumarin 6 in the rat plasma during the 2 h period was minimal (i.e., <7% under the given condition, data not shown). The uptake increased as the concentration of chitosan in the

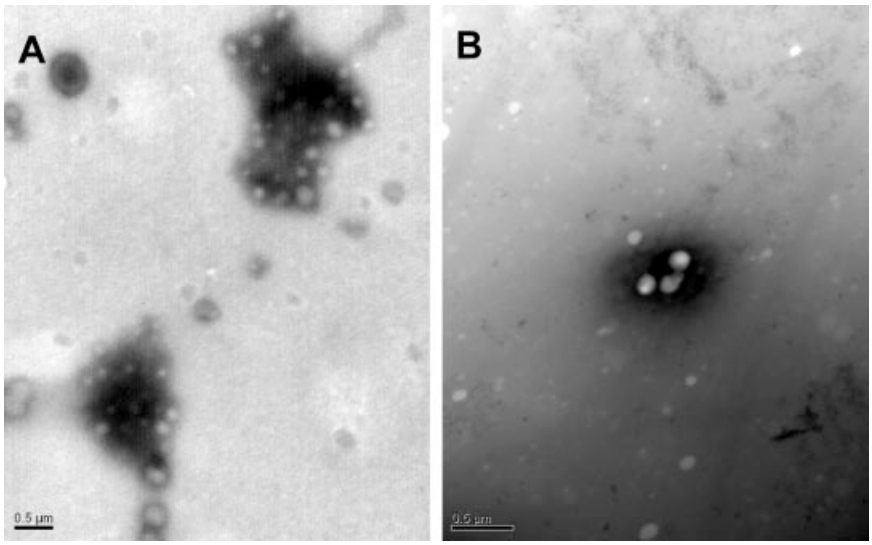

Figure 3. TEM images of chitosan modified nanoparticles (e.g., NP_3) aggregate in the plasma after pre-incubation of the nanoparticles at 37°C for 30 min with fresh mouse (CDF_1) plasma under shaking at 120 rpm (A) followed by gentle agitation of the aggregates with the glass rod for 5 min in room temperature (B).

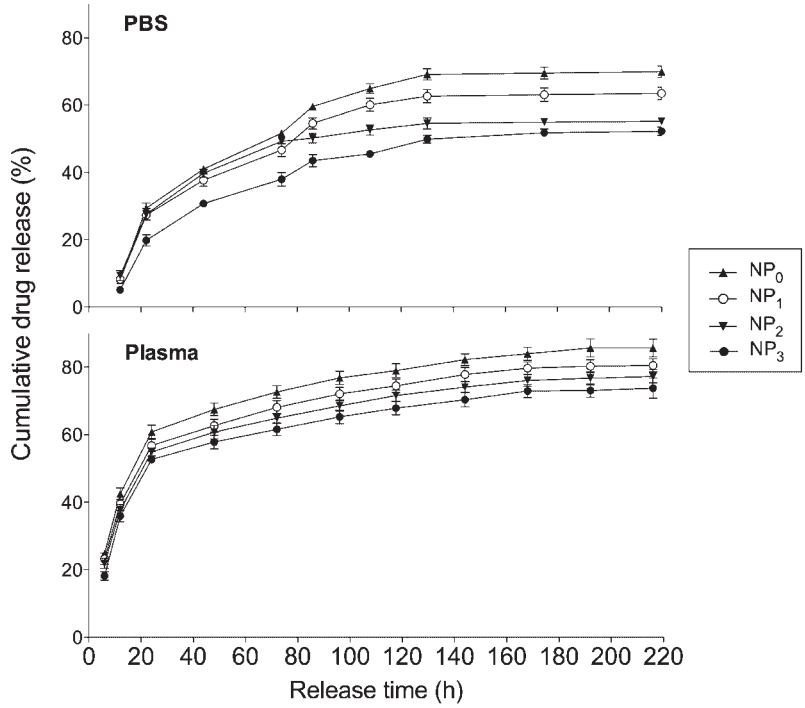

Figure 4. *In vitro* release of paclitaxel in phosphate-buffered saline (PBS, 0.01 M, pH 7.4) and SD rat plasma from surface-unmodified (NP_0, ▲), 0.3% chitosan-modified (NP_1, ○), 0.5% chitosan-modified (NP_2, ▼), and 0.7% chitosan-modified, paclitaxel-loaded PLGA nanoparticles (NP_3, ●). Each point shows the mean ± SD of three experiments.

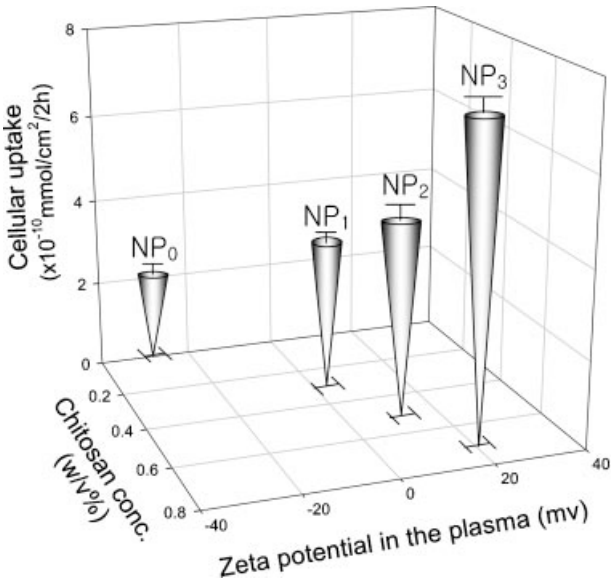

Figure 5. Cellular uptake of coumarin 6 (mean ± SD, $n = 4$) by A549 cells for 2 h from fresh mouse (CDF_1) plasma dispersions of chitosan-unmodified (NP_0), 0.3% chitosan-modified (NP_1), 0.5% chitosan-modified (NP_2), and 0.7% chitosan-modified, coumarin 6-loaded PLGA nanoparticles (NP_3) as a function of chitosan concentration in the modification solution and zeta potential of nanoparticles in the plasma.

modification solution and the zeta potential of the nanoparticles in the plasma increased. Cell membranes, especially cancer cell membranes, are usually negatively charged due to a negatively charged inner component of the cell membranes, phosphatidylserine (PS), which is translocated to the surface in the case of cancer cells.[36] Therefore, the increased uptake of chitosan-modified nanoparticles (i.e., NP_1, NP_2, and NP_3) appears to be attributable to the electrical interaction between the negative charge of the cancer cell membranes[23,24] and the positive charge of the nanoparticles, which was produced by the chitosan modification. The positive charge would enhance the efficiency of cell uptake of nanoparticles by the mechanism of clathrin-mediated endocytosis.[37] In addition, the adhesive characteristics of chitosan might have increased the adsorption of nanoparticles to the cell surface,[26,27] contributing to the increased endocytosis of nanoparticles. The results of the uptake study for chitosan-modified coumarin 6-loaded PLGA nanoparticles may be extended to a suggestion that the enhanced delivery of drugs to specific cancer cells in cancer patients may be made by chitosan modification of drug-loaded PLGA nanoparticles.

In Vitro Cytotoxicity of Paclitaxel-Loaded PLGA Nanoparticles

The cytotoxic activity of paclitaxel-loaded PLGA nanoparticles was estimated by measuring the viability of A549 cells after the incubation of the cells in mouse (CDF_1) plasma with the nanoparticles for 24, 48, and 72 h, and the results were compared with that of Taxol™ (Fig. 6). The cytotoxicity of nanoparticles increased as the incubation time increased (compare A, B, and C in Fig. 6), but were weaker than that of Taxol™. The cytotoxicity of Cremorphor EL™, a solvent of paclitaxel in Taxol™, might have contributed (at least in part) to the cytotoxicity of Taxol™.[38] The weaker cytotoxicity of nanoparticles may be attributable to the retarded release of paclitaxel from the nanoparticles. Nevertheless, cytotoxicity increased as the chitosan concentration in the modification solution increased (i.e., as the release was retarded) regardless of the incubation time ($p < 0.001$ for 24 h, and $p < 0.05$ for 48 and 72 h incubation). This may be attributable to the increased cellular uptake of nanoparticles either as a function of chitosan concentration or as zeta potential (Fig. 6).

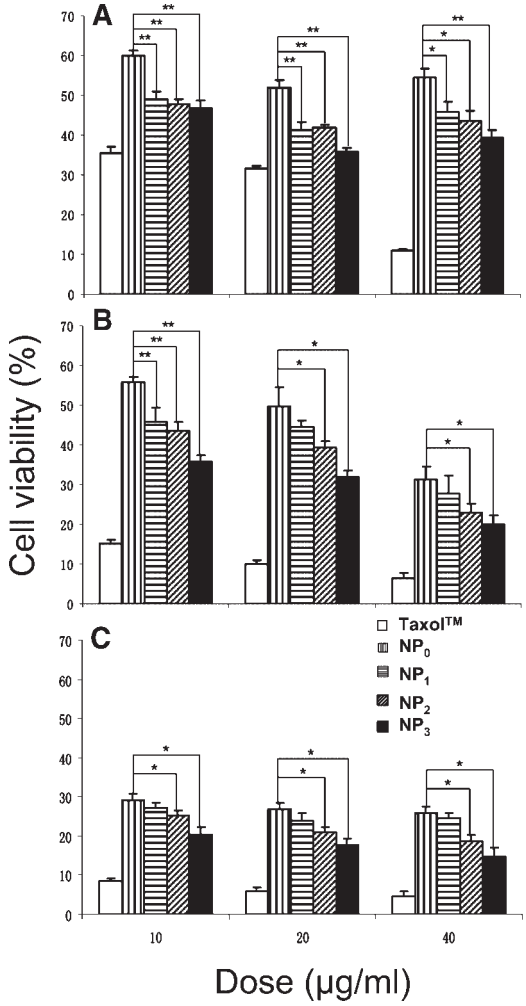

Figure 6. Cell viability of A549 cells (mean ± SD, $n = 8$) following incubation for 24 h (A), 48 h (B), or 72 h (C) with fresh mouse (CDF_1) plasma dispersions of Taxol™ (empty), surface-unmodified (NP_0, vertical stripe), 0.3% chitosan-modified (NP_1, horizontal stripe), 0.5% chitosan-modified (NP_2, diagonal stripe), and 0.7% chitosan-modified, paclitaxel-loaded PLGA nanoparticles (NP_3, filled) at paclitaxel concentrations of 10, 20, and 40 μg/mL. $^{*}p < 0.05$, $^{**}p < 0.001$.

Plasma Pharmacokinetics and Biodistribution of Paclitaxel

Plasma and tissue concentration–time profiles of paclitaxel in normal and lung metastasized mice, following tail vein administration of Taxol™, NP_0, and NP_3 at a paclitaxel dose of 10 mg/kg mouse, are shown in Figures 7 and 8, and pharmacokinetic and biodistribution parameters are summarized in Tables 2 and 3. The decline of plasma paclitaxel was slower for unmodified nanoparticles (NP_0) and slowest for the chitosan-modified nanoparticles (NP_3), compared to Taxol™, in normal and metastasized mice, suggesting the retarded elimination of paclitaxel (particularly chitosan-modified nanoparticles) from the body (Fig. 7). Retarded elimination of the drug is consistent with the well-known retarded excretion for particles, compared to drug molecules, via the urinary and biliary routes. The substantial retardation of excretion for the

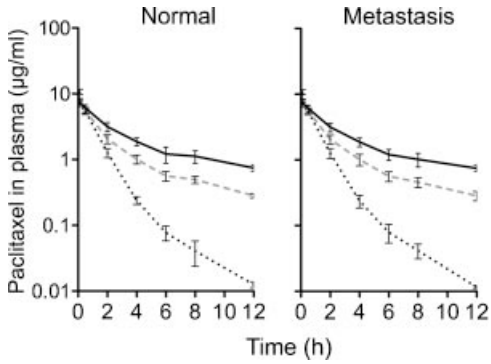

Figure 7. Plasma concentration–time profiles of paclitaxel after tail vein administration of Taxol™ (···), surface-unmodified (NP_0, - - -) and 0.7% chitosan-modified, paclitaxel-loaded PLGA nanoparticles (NP_3, —) to normal and lung metastasized CDF_1 mice at a paclitaxel dose of 10 mg/kg.

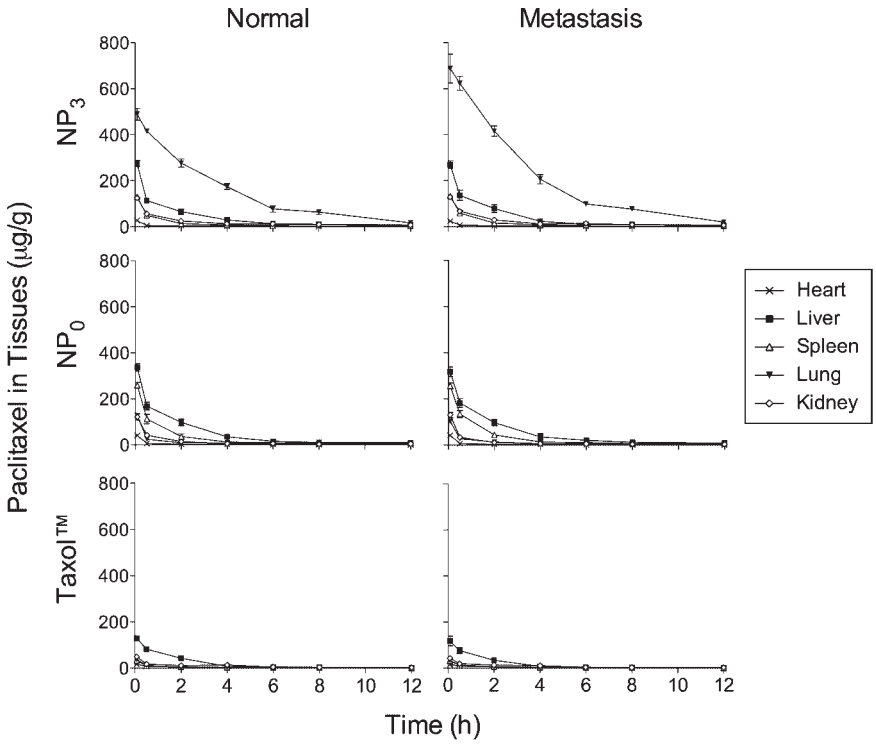

Figure 8. Tissues concentration–time profiles of paclitaxel after tail vein administration of Taxol™, surface-unmodified (NP_0,) and 0.7% chitosan-modified, paclitaxel-loaded PLGA nanoparticles (NP_3,) to normal and lung metastasized CDF_1 mice at a paclitaxel dose of 10 mg/kg.

chitosan-modified PLGA nanoparticles (NP_3) appears to be attributable to the increase in size of NP_3 in the stream of plasma to 2.7 μm (Tab. 1).

Some model-independent pharmacokinetic parameters are summarized in Table 2. The systemic plasma clearance (CL) of paclitaxel decreased in the order of Taxol™, NP_0, and NP_3 for both normal and metastasized mice, consistent with the retarded elimination of plasma paclitaxel for nanoparticles shown in Figure 7. Interestingly,

Table 2. Plasma Pharmacokinetic Parameters of Paclitaxel Following Tail Vein Administration of Taxol™, NP_0, and NP_3 to Normal and Lung Metastasized CDF_1 Mice (n = 4) at a Paclitaxel Dose of 10 mg/kg

	Normal Mice			Lung Metastasis Mice		
Parameters	Taxol™	NP_0	NP_3	Taxol™	NP_0	NP_3
CL (L/h/kg)	0.88	0.50	0.31	0.91	0.53	0.33
Vd_{ss} (L/kg)	0.92	1.93	2.55	0.96	2.01	2.68

Each value was calculated based on the mean plasma concentrations of four different mice.

the distribution volume (Vd_{ss}) of paclitaxel generally increased in the order of Taxol™, NP_0, and NP_3, suggesting that the body distribution of paclitaxel is improved by incorporation into nanoparticles, particularly into the chitosan-modified nanoparticles (e.g., NP_3). In order to confirm this finding, the biodistribution of paclitaxel from Taxol™, NP_0, and NP_3 to various organ tissues was investigated.

Figure 8 shows the paclitaxel concentration–time profiles in various tissues of normal and metastasized mice. The profile differed greatly depending on the formulations and tissues. In the case of Taxol™, the liver demonstrated the highest drug concentration, which was followed by the kidney in both types of mice. In the case of NP_0, the drug level was highest in the liver, followed by the spleen. In the case of NP_3, the level was highest in the lung compared to other tissues, followed by the liver, particularly in mice with metastasis.

The AUC_{tissue} values for NP_0 and NP_3 were generally larger than those from Taxol™ in both types of mice (Tab. 3), consistent with the generally larger Vd_{ss} for these formulations

Table 3. The AUC and Tissue Distribution Index of Paclitaxel in Various Tissues Following Tail Vein Administration of Taxol™, NP_0, and NP_3 to Normal and Lung Metastasized CDF_1 Mice (n = 4) at a Paclitaxel Dose of 10 mg/kg

	Normal Mice						Metastasis Lung Mice					
	AUC[a] (μg h/mL)			Distribution Index[b]			AUC[a] (μg h/mL)			Distribution Index[b]		
Tissue	Taxol™	NP_0	NP_3	Taxol™	NP_0	NP_3	Taxol™	NP_0	NP_3	Taxol™	NP_0	NP_3
Plasma	11.4	18.7	24.6	1	1	1	10.3	17.3	24.2	1	1	1
Heart	30.2	43.6	37.2	2.6	2.3	1.5	31.3	42.5	34.6	3.0	2.5	1.4
Liver	232.4	569.8	445.6	20.4	30.5	18.1	201.7	581.6	461.3	19.6	33.6	19.1
Spleen	50.7	359.8	165.6	4.4	19.2	6.7	57.2	380.5	190.6	5.6	22.0	7.9
Lung	54.6	117.2	1768.5	4.8	6.3	71.9	55.4	114.5	2416.5	5.4	6.6	99.9
Kidney	102.7	147.6	235.9	9.0	7.9	7.9	95.4	131.5	246.3	9.3	7.6	10.2

[a]All AUC values were calculated using mean paclitaxel concentrations of four different mice at each sampling time point.
[b]Distribution indexes were calculated by $AUC_{tissues}/AUC_{plasma}$ for each formulation, respectively.

(Tab. 2). The most distinct increase was observed for the AUC_{lung} of NP_3, which demonstrated 32.4- and 43.6-fold increases compared to the AUC_{lung} of Taxol™ in normal and metastasized mice, respectively. For NP_0, only a 2-fold increase in the AUC_{lung} could be achieved.

The efficiency of drug delivery to a specific tissue can be expressed by the ratio of the drug dose in the tissue and the drug dose in the blood circulate (i.e., distribution index in Tab. 3), which can be calculated by the AUC ratio between tissues and plasma (i.e., $AUC_{tissue}/AUC_{plasma}$). The distribution index from unmodified PLGA nanoparticles, NP_0, for the liver and spleen was larger compared to Taxol™ and other tissues. This is consistent with the hypothesis that nanoparticles are removed from circulation by the reticuloendothelial system (RES) organs (e.g., liver and spleen) through phagocytosis by Kupper cells (liver) and macrophages (spleen).[39] With the chitosan-modification of the nanoparticles, a dramatic increase was observed in the distribution index of the drug to the lung. In normal mice, the index was 4.8 for Taxol™ and 6.3 for NP_0, but 71.9 for NP_3, exhibiting a 15.0-fold increase for NP_3 compared to Taxol™. Therefore, the increase in distribution to the lung appears to be responsible for the increased Vd_{ss} of the drug for NP_3 in Table 2. Despite the distinct increase in distribution to the lung, distribution indexes for NP_3 decreased or remained constant for the other tissues of organs. It may indicate that chitosan modification did not mediate the uptake of nanoparticles by the RES (opsonization).[40] These results indicate the preferential delivery of drug to the lungs is feasible by the administration of paclitaxel-loaded PLGA nanoparticles.

A similar tendency was observed for the distribution index in the metastasized mice. Most importantly, the distribution index to the lung from NP_3 was larger than those to the other tissues. The index was 5.4 for Taxol™ and 6.6 for NP_0, but 99.9 for NP_3, exhibiting an 18.5-fold increase for NP_3 compared to Taxol™. The distribution index of NP_3 to the metastasis lung was even larger than that to the lung of normal mice (i.e., 71.9 vs. 99.9). In contrast, the distribution index to the heart was reduced for NP_3 compared to Taxol™ (i.e., 3.0 vs. 1.4), and the indexes to the liver, spleen and kidney were comparable between Taxol™ and NP_3, suggesting an advantage of NP_3 over Taxol™ in avoiding unnecessary side effects of paclitaxel on the heart.[13] The preferential distribution of paclitaxel to the metastasized lung with unchanged or reduced distribution of the drug to other tissues suggests the potential of chitosan-modified, paclitaxel-loaded PLGA nanoparticles as a promising delivery system for paclitaxel to the metastasized lung under the assumption that transient aggregates of nanoparticles.

The underlying mechanism(s) of the lung accumulation of paclitaxel from NP_3 was not pursued in detail in the present study, but the transient formation of large nanoparticle aggregates (e.g., 2.7 μm, Tab. 1) in contact with plasma proteins during circulation, followed by enhanced entrapment of large aggregates by the lung capillaries, might represent the principal mechanisms. This hypothesis is based on the fact that

large size aggregates (e.g., 2.0–10.0 μm[41]) are efficiently trapped in the capillary bed of the normal or tumor vasculature of the lung. In addition, electrical interaction between the positively charged nanoparticles (e.g., NP_3) and negatively charged endothelial cells of the tumor vasculature might have potentiated the accumulation of NP_3 aggregates in the lung tumor capillaries.[42] The negative charge of endothelial cells of the tumor vasculature appears to be attributable to the over-expression of negatively charged surface molecules, for example, anionic phospholipids, glycoproteins and proteoglycans.[43–48] This hypothesis is supported by the delivery of cationic liposomes to microvessels of solid tumors.[22]

The potential advantage of chitosan-modified nanoparticles over the permanent microparticulate drug delivery systems may exist in that they form transient aggregates of nanoparticles in the plasma, as confirmed by their reversible size change in the plasma. Transient aggregates of microsize are likely to be efficiently entrapped in the lung capillary vasculature via above-mentioned mechanisms, thereby leading to temporal accumulation of the aggregates in the lung capillary.

Accumulation of microparticles may result in the embolization of the vasculature. However, the degree of embolization from the transient aggregates of nanoparticles will not be so serious compared to permanent microparticles, because the aggregates may be dissociated to original size after the temporal accumulation in the capillary. Therefore, potential toxicity problems of permanent microparticles in association with embolization would be avoided at least in part by the transient aggregates. Loose aggregation and dissociation *in vivo* has also been observed for cationic liposomes.[49]

CONCLUSION

In this study, chitosan-modified paclitaxel-loaded PLGA nanoparticles were prepared. The surface charge of PLGA nanoparticles could be modified from negative to positive by treatment of the surface of PLGA nanoparticles with the chitosan solution. The size of nanoparticles increased dramatically in plasma as the concentration of chitosan in the modification solution increased (e.g., 2.7 μm for 0.7% chitosan-modified nanoparticles, NP_3). Most importantly, a preferential accumulation of paclitaxel in the lung could be achieved both in normal and lung-metastasized mice. For example, a distribution index (i.e., AUC_{lung}/AUC_{plasma}) of 99.9 was obtained following tail vein administration of NP_3 into the metastasized mice at a paclitaxel dose of 10 mg/kg. Increased size of nanoparticles due to transient formation of aggregates in the plasma, substantial retardation of paclitaxel in the nanoparticles, and electrical interaction between the positively charged nanoparticle surfaces and negatively charged endothelium of lung tumor vasculature appear to be responsible for the lung-specific accumulation of paclitaxel. Although the *in vitro* cytotoxicity of paclitaxel was decreased with the nanoparticles, the distinct *in vivo* accumulation of nanoparticles exclusively in the lung, the enhanced *in vitro* uptake of nanoparticles into cancer cells, and, possibly, the moderate *in vivo* release of paclitaxel[50] suggest the feasibility of chitosan-modified, paclitaxel-loaded poly lactic-*co*-glycolic acid (PLGA) nanoparticles as a lung-specific delivery system for paclitaxel in lung cancer patients. Most importantly, transient aggregates of nanoparticles in the present study may not expected to evoke serious embolization-related toxicity problem compared to permanent micro-particulate drug delivery systems, suggesting potential advantage of this approach in terms of *in vivo* safety issues.

ACKNOWLEDGMENTS

This study was supported by a grant from the Korean Science and Engineering Foundation (KOSEF) through the National Research Laboratory Program founded by the Ministry of Science and Technology (ROA-2006-000-10290-0).

REFERENCES

1. Parkin DM, Bray F, Ferlay J, Pisani P. 2005. Global cancer statistics. CA Cancer J Clin 55:74–108.
2. Thomas CRJ, Williams TE, Cobos E, Turrisi AT. 2001. Lung cancer. In: Lenhard REJ, Osteen RT, Gansler T, editors. Clinical oncology. Atlanta, GA: American Cancer Society. pp 269–295.
3. Eldem T, Speiser P, Hincal A. 1991. Optimization of spray-dried and -congealed lipid micropellets and characterization of their surface morphology by scanning electron miscopy. Pharm Res 8:47–54.
4. Saralidze K, Van Hooy-Corstjens CS, Koole LH, Knetsch ML. 2007. New acrylic microspheres for arterial embolization: Combining radiopacity for

precise localization with immobilized thrombin to trigger local blood coagulation. Biomaterials 28: 2457–2464.
5. Darwis Y, Kellaway IW. 2001. Nebulization of rehydrated freeze-dried beclomethasone dipropionate liposomes. Int J Pharm 215:113–121.
6. Kellaway IW, Farr SJ. 1990. Liposomes as drug delivery systems to the lung. Adv Drug Deliv Rev 5:149–161.
7. Johnson KA. 1997. Preparation of peptide and protein powders for inhalation. Adv Drug Deliv Rev 26:3–15.
8. Kitamura H, Ichinose S, Hosoya T, Ando T, Ikushima S, Oritsu M, Takemura T. 2007. Inhalation of inorganic particles as a risk factor for idiopathic pulmonary fibrosis—Elemental microanalysis of pulmonary lymph nodes obtained at autopsy cases. Pathol Res Pract 203:575–585.
9. Klonne DR, Dodd DE, Losco PE, Troup CM, Tyler TR. 1998. Pulmonary fibrosis produced in F-344 rats by subchronic inhalation of aerosols of a 4000 molecular weight ethylene oxide/propylene oxide polymer. Fundam Appl Toxicol 10:682–690.
10. Brannon-Peppas L, Blanchette JO. 2004. Nanoparticle and targeted systems for cancer therapy. Adv Drug Deliv Rev 56:1649–1659.
11. Mao Y, Lim LY. 2005. Paclitaxel-loaded PLGA nanoparticles: Potentiation of anticancer activity by surface conjugation with wheat germ agglution. J Control Release 108:244–262.
12. Yamamoto H, Kuno Y, Sugimoto S, Takeuchi H, Kawashima Y. 2005. Surface-modified PLGA nanosphere with chitosan improved pulmonary delivery of calcitonin by mucoadhesion and opening of the intercellular tight junctions. J Control Release 102: 373–381.
13. Lehoczky O, Bagaméri A, Udvary J, Pulay T. 2001. Side-effects of paclitaxel therapy in ovarian cancer patents. Eur J Gynaecol Oncol 22:81–84.
14. Sharma S, Ganesh T, Kingston DG, Bane S. 2007. Promotion of tubulin assembly by poorly soluble taxol analogs. Anal Biochem 360:56–62.
15. Lundberg BB, Risovic V, Ramaswamy M, Wasan KM. 2006. A lipophilic paclitaxel derivative incorporated in a lipid emulsion for parenteral administration. J Control Release 86:93–100.
16. Seow WY, Xue JM, Yang YY. 2007. Targeted and intracellular delivery of paclitaxel using multifunctional polymeric micelles. Biomaterials 28: 1730–1740.
17. Straubinger RM, Balasubramanian SV. 2005. Preparation and characterization of taxane-containing liposomes. Methods Enzymol 391:97–117.
18. Jackson JK, Hung T, Letchford K, Burt HM. 2007. The characterization of paclitaxel-loaded microspheres manufactured from blends of poly(lactic-co-glycolic acid) (PLGA) and low molecular weight diblock copolymers. Int J Pharm 342:6–17.
19. Hamada H, Ishihara K, Masuoka N, Mikuni K, Nakajima N. 2006. Enhancement of water-solubility and bioactivity of paclitaxel using modified cyclodextrins. J Biosci Bioeng 102:369–371.
20. Fulzele SV, Satturwar PM, Dorle AK. 2003. Study of the biodegradation and in vivo biocompatibility of novel biomaterials. Eur J Pharm Sci 20:53–61.
21. Ding SJ. 2007. Biodegradation behavior of chitosan/calcium phosphate composites. J Non-Cryst Solids 353:2367–2373.
22. Thurston G, McLean JW, Rizen M, Baluk P, Haskell A, Murphy TJ, Hanahan D, McDonald DM. 1998. Cationic liposomes target angiogenic endothelial cells in tumors and chronic inflammation in mice. J Clin Invest 101:1401–1413.
23. Gallez D. 1984. Cell membranes after malignant transformation. Part I. Dynamic stability at low surface tension. J Theor Biol 111:323–340.
24. Mehrishi JN. 1969. Effect of lysine polypeptides on the surface charge of normal and cancer cells. Eur J Cancer 5:427–435.
25. Ungewickell EJ, Hinrichsen L. 2007. Endocytosis: Clathrin-mediated membrane budding. Curr Opin Cell Biol 19:1–9.
26. He P, Davis SS, Illum L. 1998. In vitro evaluation of the mucoadhesive properties of chitosan microspheres. Int J Pharm 168:75–88.
27. Pavinatto FJ, Pavinatto A, Caseli L, Santos DS, Jr., Nobre TM, Zaniquelli ME, Oliveira ON, Jr. 2007. Interaction of chitosan with cell membrane models at the air-water interface. Biomacromolecules 8:1633–1640.
28. Dong Y, Feng SS. 2005. Poly(D,L-lactide-co-glycolide)/montmorillonite nanoparticles for oral delivery of anticancer drugs. Biomaterials 26: 6068–6076.
29. Furumoto K, Ogawara K, Nagayama S, Takakura Y, Hashida M, Higaki K, Kimura T. 2002. Important role of serum proteins associated on the surface of particles in their hepatic disposition. J Control Release 83:89–96.
30. Fang C, Shi B, Pei YY. 2005. Effect of MePEG molecular weight and particle size on in vitro release of tumor necrosis factor-alpha-loaded nanoparticles. Acta Pharmacol Sin 26:242–249.
31. Kim SC, Yu J, Lee JW, Park ES, Chi SC. 2005. Sensitive HPLC method for quantitation of paclitaxel (Genexol®) in biological samples with application to preclinical pharmacokinetics and biodistribution. J Pharm Biomed Anal 39:170–176.
32. Sakurai F, Terada T, Maruyama M, Watanabe Y, Yamashita F, Takakura Y, Hashida M. 2003. Therapeutic effect of intravenous delivery of lipoplexes containing the interferon-β gene and poly I: Poly C in a murine lung metastasis model. Cancer Gene Ther 10:661–668.
33. Lacasse FX, Filion MC, Phillips NC, Escher E, McMullen JN, Hildgen P. 1998. Influence of surface

properties at biodegradable microsphere surfaces: Effects on plasma protein adsorption and phagocytosis. Pharm Res 15:312–317.
34. Mauduit J, Vert M. 1993. Poly(lactic acid)/poly(glycolic acid) homo- and copolymers and sustained drug delivery. STP Pharma Sci 3:197–212.
35. Cai Q, Shi G, Bei J, Wang S. 2003. Enzymatic degradation behavior and mechanism of poly(lactide-co-glycolide) foams by trypsin. Biomaterials 24:629–638.
36. Ran S, Downes A, Thorpe PE. 2002. Increased exposure of anionic phospholipids on the surface of tumor blood vessels. Cancer Res 62:6132–6140.
37. Harush-Frenkel O, Debotton N, Benita S, Altschuler Y. 2007. Targeting of nanoparticles to the clathrin-mediated endocytic pathway. Biochem Biophys Res Commun 353:26–32.
38. Fjällskog ML, Frii L, Bergh J. 1993. Is Cremophor EL, solvent for paclitaxel, cytotoxic? Lancet 342: 1428.
39. Patel HM. 1992. Serum opsonin and liposomes: Their interaction and opsonophagocytosis. Crit Rev Ther Drug Carrier Syst 9:39–3990.
40. Moghimi SM, Hunter AC, Murray JC. 2001. Long-circulating and target-specific nanoparticles: Theory and practice. Pharmacol Rev 53:283–318.
41. Lu B, Zhang JQ, Yang H. 2003. Nonphospholipid vesicles of carboplatin for lung targeting. Drug Deliv 10:87–94.
42. Denekamp J. 1990. Vascular attack as a therapeutic strategy for cancer. Cancer Metastasis Rev 9: 267–282.
43. Augustin HG, Braun K, Telemenakis I, Modlich U, Kuhn W. 1995. Ovarian angiogenesis phenotypic characterization of endothelial cells in a physiological model of blood vessel growth and regression. Am J Pathol 147:339–351.
44. Augustin HG, Kozian DH, Johnson RC. 1994. Differentiation of endothelial cells: Analysis of the constitutive and activated endothelial cell phenotypes. Bioessays 16:901–906.
45. Iozzo RV, San-Antonio JD. 2001. Heparan sulfate proteoglycans: Heavy hitters in the angiogenesis arena. J Clin Invest 108:349–355.
46. Ran S, Downes A, Thorpe PE. 2002. Increased exposure of anionic phospholipids on the surface of tumor blood vessels. Cancer Res 62:6132–6140.
47. Ran S, Thorpe PE. 2002. Phosphatidylserine is a marker of tumor vasculature and a potential target for cancer imaging and therapy. Int J Radiat Oncol Biol Phys 54:1479–1484.
48. Kirkpatrick AP, Kaiser TA, Shepherd RD, Rinker KD. 2003. Biochemical mediated glycocalyx modulation in human umbilical vein endothelial cells (HUVEC). Summer Bioengineering Conference: 25–29.
49. Ishiwata H, Suzuki N, Ando S, Kikuchi H, Kitagawa T. 2000. Characteristics and biodistribution of cationic liposomes and their DNA complexes. J Control Release 69:139–148.
50. Win KY, Feng SS. 2006. In vitro and in vivo studies on vitamin E TPGS-emulsified poly(D,L-lactic-co-glycolic acid) nanoparticles for paclitaxel formulation. Biomaterials 27:2285–2291.